STRAIN HARDENING EFFECTS ON THE WARM PRESTRESSING OF FERRITIC STEELS

B.de Jong*

The improvement of the low temperature toughness level of ferritic steels by warm prestressing (WPS) is discussed.
A model is proposed which incorporates the cumulative strain hardening effects by completely simulating a WPS-cycle using an elasto-plastic finite element program. With the Ritchie, Knott and Rice cleavage fracture criterion, the load at which the low temperature stress distribution becomes critical and cleavage occurs, is determined. The model is verified by executing some experiments on standard toughness SENB specimens. The material used in this investigation is a fine grain carbon manganese ferritic pressure vessel steel.

INTRODUCTION

Warm prestressing (WPS) is a process which can improve the low temperature toughness level of ferritic steels. A WPS-cycle generally consists of prestressing a cracked structure at an upper shelf temperature, after which it is unloaded and cooled to a temperature below the ductile-brittle transition temperature. After reloading at this temperature the toughness level may be increased considerably. This load-unload-cool-fracture-cycle (LUCF) is illustrated in Fig. la. Beneficial effects on low temperature toughness are also obtained if the material is only partially unloaded or not unloaded at all. See for a LCF-cycle Fig. lb. This WPS-phenomenon may occur in a number of practical situations, for example, as a consequence of an accidental loss of coolant in a pressurised water reactor circuit or when hydrotesting pressure vessels and storage tanks for

* Currently employed at Shell Internationale Petroleum Maatschappij B.V. 's Gravenhage.

cryogenic liquids.
Nichols (1) suggested three possible reasons why the low temperature toughness level can be increased by WPS: notch blunting, increase of yield strength locally as a result of work hardening at the crack tip and the introduction of residual compressive stresses ahead of a crack tip. Harrison and Fearnehough (2) tested single edge notch bend specimens (SENB) of a carbon-manganese steel, which had been warm prestressed at ambient temperature and fractured at - 196°C. They found that LCF-cycles showed better toughness improvements than LUCF-cycles, from which they concluded that the beneficial effect of preloading should be attributed to the modification of the stress pattern below the notch as a result of yielding, and not necessarily to the introduction of any residual compressive stress. Reverse plastic flow occcuring at unloading apparently influences this beneficial stress pattern in a negative sense.
A quantitative model describing the WPS-phenomenon was proposed by Koshiga (3). He assumed fracture to occur when the plastic zone size in tension reaches a critical value. To estimate the plastic zone size he used the Dugdale model, assuming elastic-ideally plastic material behaviour. Despite the simplicity of the model, reasonable agreement was found between experimental and calculated data.
A more advanced quantitative description of the WPS - phenomenon was proposed by Chell and Vitek (4), Chell et al (5). The theory is based on a modified J-integral, called the "J_e-integral", which differs from the ordinary path independent J-integral as it is evaluated only from elastic strains and distortions. This modified integral has the physical meaning of the force on all singularities (e.g. dislocations) enclosed by the contour of integration and thus will be path dependent if, by taking another contour, singularities are omitted or included. Fracture is presumed to occur when the force on the mobile dislocations reaches a critical value J_c. Thus the contour of integration has to include these mobile dislocations and to exclude the immobilized ones. J_e can be expressed in terms of "displacement discontinuities", which in turn can be expressed in terms of the stress intensity factors resulting from any applied loads.
Chell used the principle of superposition when assessing the final value of the displacement discontinuities after the loading, unloading and reloading steps. Although his expression proposed for these displacement discontinuities was derived for linear elastic-ideally plastic materials, the predicted stress intensity factors at failure were in close agreement with

experimentally determined values.
Curry (6) derived an alternative model which permits quantitative predictions of WPS-effects. The basis of this model is the Ritchie, Knott and Rice (RKR) cleavage fracture criterion for ferritic steels (7), which states that cleavage occurs when the maximum principal stress ahead of a stress concentrator exceeds a critical value (σ_f) over a microstructurally significant size scale (X_o^f). For plane strain slip-induced cleavage fracture it appears that the critical stress σ_f is largely temperature and strain rate independent. Curry and Knott (8) investigated the critical microstructural distance X_o and they found that there exists a linear relation between this distance and the ferrite grain size, X_o being approximately 2-3 times the grain size with a minimum value of about 180 μm.
Curry (6) suggests that the stress distribution ahead of the crack tip for loading at low temperature following WPS can be obtained by superposition of the appropriate stress distributions for loading, unloading and reloading. This is a similar approach to that used by Chell, who superimposed displacement discontinuities. Although Curry took account of the strain hardening effect within each separate step by means of a strain hardening exponent, little difference was found between values predicted by him and the ones of Chell.

PROPOSED THEORY

From previous work it is accepted that the stress distribution ahead of a crack mainly causes the appearance of cleavage fracture. This stress distribution at the lower shelf temperature depends upon the increase of yield stress as a result of hardening and a decreased temperature. In addition to this the residual stresses which are present before the start of the reloading also affect the stress distribution.
In order to improve upon previous modelling, we have considered the effects that cumulative strain hardening, caused by loading and unloading at the upper shelf temperature, have upon the low temperature stress distribution ahead of the crack tip at reloading. In recent studies carried out at Twente University of Technology and discussed herein, this is realized by simulating the entire WPS-cycle with an elasto-plastic finite element program. With the RKR-criterion, the load at which the low temperature stress distribution becomes critical and cleavage occurs, is determined.

NUMERICAL APPROACH

As the theory requires the use of an elasto-plastic finite element program a short description is given first of the EPFEM-program, developed at the Twente University of Technology. The program can compute plane stress, plane strain and axisymmetric problems taking into account physical and geometrical nonlinearities. The frame of reference is a Cartesian, respectively cylindrical updated Lagrangian one. The incremental tangent stiffness method applied, comprises incremental constitutive equations, relating the Jaumann increments of Cauchy's "true" stresses to the increments of strains.
The von Mises yield criterion has been used along with the rule of normality of the incremental plastic strain tensor with respect to the yield surface.
To describe kinematic and combined kinematic and isotropic hardening the fraction model of Besseling (9) has been implemented. The isotropic hardening of the material has been taken a function of the total plastic work dissipation per unit deformed volume.
The elements are 4-node isoparametric quadrilateral, with a linear displacement field and four integration points. Following suggestions made by Nagtegaal et al (10) a modified strain increment has been used in the plane strain and axisymmetric formulation to avoid difficulties arising from enforced kinematic constraints on the modes of deformation. The incremental tangent stiffness solutions are corrected by an iterative corrective load procedure based upon the Newton-Raphson method. A further refinement, which has been built in to correct the stresses, is based upon the division of the total strain increment into a number of smaller ones. In this way it is possible to improve the computed resistance, produced by the elements by an incremental integration procedure. The program offers the possibility to prescribe the behaviour of each group of elements in terms of linear elastic and elastic-plastic infinitesimal deformations or elastic-plastic finite deformations.
To enable verification, the present study was confined to SENB-specimens.
In order to obtain close accuracy with the minimum of calculation effort, the element mesh has been divided into sections - a linear elastic subnet with plane stress elements; an elasto-plastic mainnet with plane strain elements which consists of an infinitesimal deformation part and a finite deformation part. See Fig. 2.
The loading step at the upper shelf (=ambient)

temperature has been simulated by incrementally applying the desired preload on the mesh described above.
In view of the large deformations that occur near the crack tip a true stress versus natural strain curve has been used. This curve had been obtained by performing tensile tests on initially necked specimens.
To find the proper one-dimensional stress during necking of the tensile specimens, the Bridgman-correction procedure has been used (11). Using a finite element computation this Bridgman corrected strain hardening curve has been verified. In the finite element program this corrected curve has been applied in multi linearized shape.
Due to a lack of experimental data relating to large deformation hardening properties in compression - in particular with regard to the Bauschinger effect - one isotropic hardening fraction has been used.
Since reverse plastic deformation occurs near the crack tip, the unloading step has been simulated by incrementally removing the preload.
The cooling process has been simulated by replacing the upper shelf material data by the lower shelf ones in the program. The low temperature material properties have been determined by tensile tests at this temperature.
The reloading step at the lower shelf temperature has been simulated by incrementally applying the load. The failure event has been determined with the RKR-cleavage criterion. The calculation has been stopped and the failure load determined when it had been ascertained that the maximum principal stress perpendicular to the plane of the crack exceeds the critical value σ_f over the characteristic distance X_o.
Since the yield stress in the finite element computations is dependent on the cumulative specific plastic work, the question arises whether the plastic work, resulting from the loading and unloading at the upper shelf temperature, may be used as the initial value for the amount of hardening in the reloading step at the lower shelf temperature. With some WPS-experiments on initially necked tensile bars, it has been verified that this specific plastic work must indeed be transferred from the upper shelf steps to the lower shelf step.
The fracture stress σ_f and characteristic distance X_o for the material used, have been determined by a combined numerical and experimental investigation. By using standard 3-point bending test pieces as described in BS-5447, two low temperature K_{Ic} - values have been determined at different temperatures. By plotting the numerically determined values of the principal stress ahead of the crack at fracture of these test pieces as function of the distance to the crack tip, the point of

intersection of these plots determines the critical stress σ_f and the characteristic distance X_o.

RESULTS

The material that has been used for the tests and computations is a high strenght low alloy ferritic carbon-manganese pressure vessel steel (TTSt E36). The ferrite grain size is 8-9 μm.

The chemical composition of the steel is (in wt. %)

C	Si	Mn	P	S	Al	Nb
0.17	0.34	1.50	0.007	0.008	0.034	0.033

Tensile tests

The general procedure for performing tensile tests and converting the autographically recorded results into Bridgman corrected strain hardening curves may be summarised as follows.
The cylindrical tensile specimens were provided with an axial curvature as shown in Fig. 3. At the position where the initial diameter has a minimum size, necking occurs. During a test the load was recorded against the change of the smallest diameter of the specimen. For the tests that were to be executed at low temperatures, a cooling device was used, which operated with evaporating liquid nitrogen. A COD-clip gauge for use in cryogenic environments was modified, so that running measurements of the smallest neck-diameter were possible at low temperatures. The natural strain in the axial direction was determined from the incompressibility rule for plastic deformation. Thus the natural strain (denoted by $\ln(l/l_0)$) equals $\ln(A_0/A)$, where A_0 is the initial area and A the current area measured in the neck. From these tests the average value of the stress across the neck, being the load F divided by the current area of the neck A, was plotted against the natural strain measured in the neck of the specimen. The strain hardening curve derived fits in with the lower yield stress of the material, neglecting the upper yield stress.
Due to the non-uniform stress state at the neck, the average stress across the neck had to be multiplied by a correction factor as given by Bridgman (11) to determine

the approximated flow stress. The resulting uniaxial stress-strain curves have been given in Figs. 4 and 5. These stress-strain curves have been used in the EPFEM-program.

Warm-prestressed tensile tests

To check the above assumption with respect to the transfer of the specific plastic work, some WPS-experiments have been performed on tensile bars.
Initially necked tensile specimens (Fig. 3) were loaded at ambient temperature to predetermined values. This prestressing was carried out under controlled loading conditions. The load was applied in one minute, kept constant for ten minutes and removed in one minute. The load and change in diameter were recorded. After cooling, the specimens were subjected to tensile tests. The results are presented in Figs. 4 and 5. The plots indicate, that the shape of the strain hardening curves generally remains the same, whereas the initial yield stress increases after WPS.

Some experimental values of the prestress tests are presented in TABLE 1.

Specimen	Prestress load [MPa]	Test temp. [°C]	Yield stress original [MPa]	Yield stress after WPS [MPa]
W1	489	-150	681	773
W2	532	-150	681	810
W3	628	-150	681	890
X1	462	-120	583	652
X2	515	-120	583	701
X3	602	-120	583	781

TABLE 1 - Prestress data of tensile tests.

The WPS-tests on tensile specimens W1 and X1 have been simulated with finite element computations, using the Bridgman corrected strain hardening curves.
The specific plastic work, resulting from the loading and unloading at the upper shelf temperature was used as initial value for the amount of hardening in the reloading step at the lower shelf temperature. The

numerical and experimental (uncorrected) strain hardening curves are shown in Fig. 6.
Although the numerically determined yield stresses deviate from the experimental values, reasonable agreement is found between the experimental and the numerical stresses at greater strains. The deviations near the yield stress level may be attributed to the fact that in experimental situations prestressing at ambient temperature above the yield stress prohibits flow during any successive tensile test. This is not reflected in the finite element approach, in which strain hardening curves have been used which always allow for flowing, even for the preloaded material.
Since the strains at the characteristic distance from the crack tip will not be small, the present assumption has sufficient accuracy for the objectives being pursued.

K_{Ic}-tests

The fracture stress σ_f and characteristic distance X_o have been determined as follows.
Three K_{Ic}-tests were performed at -150°C which gave an average K_{Ic}-value of 1472 $N/mm^{3/2}$. Four other K_{Ic}-tests were performed at -120°C which however failed to give valid K_{Ic}-values since K_{max} exceeded K_q by more than 10%.
Two calculations were performed with EPFEM in order to determine the maximum principal stress distribution ahead of the crack tip at the moment of failure for both sets of tests. As the K_q-values, measured at -120°C were invalid, combined with the fact that at -150°C K_q coincided with K_{max}, it was decided to use the stress distributions belonging to K_{max} for the determination of σ_f and X_o. (See Fig. 7). It follows from this figure that σ_f =1611 N/mm^2 and X_o = 162 μm. These results have been used in further calculations.

Warm prestress tests with SENB-specimens

Three different types of WPS-experiments have been executed, indicated with the capitals B, C and E. They are summarised in TABLE 2. The WPS-procedure was similar to the procedure used for the tensile specimens. The prestressing was carried out under controlled loading conditions and the testing machine was adjusted so that the prestress load was attained in one minute, kept

constant for ten minutes and removed in one minute. The load was recorded as a function of the clip-gauge output. After WPS, the SENB-specimens were subjected to a fracture toughness test at the desired temperature in accordance with BS-5447. The results are shown in the table. The last column is added to enable comparison of the K_f-values at fracture after WPS with the fracture toughness of unprestressed specimens at the same test temperature.

specimen	prestress load K_I [N/mm$^{3/2}$] actual	average	test temp. [°C]	fracture load after WPS K_f [N/mm$^{3/2}$] actual	average	fracture toughness [N/mm$^{3/2}$]
B1	1841			2074		
B2	1813	1843	-150	2026	2055	1472
B3	1874			1775		
B4	1844			2343		
C1	1854			2179		
C2	1862	1859	-120	2501	2401	1856
C3	1862			2523		
E1	1319			1720		
E2	1288	1308	-150	1578	1586	1472
E3	1318			1460		

TABLE 2 - Warm prestress results of SENB-tests.

As can be observed from the last three columns, all the experiments, except experiment E3, yielded a positive WPS-effect. If the average K_f-value of experiments E1 through E3 is considered, then a positive WPS-effect results, though the prestress K_I was lower than K_{Ic} at -150°C.
One finite element computation has been made to simulate the loading and subsequent unloading at ambient temperature to a K_I-value of 1851 N/mm$^{3/2}$, corresponding to the average K_I-value as measured in tests B1-B4 and C1-C3.
The results of the present theory are presented in column 5 of TABLE 3. For comparison the results according to the theories of Chell and Curry have been added, the latter results having been based upon material data as given in TABLE 4.

test symbol	prestress load K_I[N/mm$^{3/2}$]	test temp [°C]	fracture load after WPS K_f [N/mm$^{3/2}$] experimental	present theory	Chell	Curry
B	1843	-150	2055	2039	2148	2007
C	1859	-120	2401	2325	2316	2062
E	1308	-150	1586	1755	1804	1702

TABLE 3 - Results of WPS-tests and computations.

temp. [°C]	yield stress [MPa]	strain hardening exponent N	fracture toughness K_{Ic}[N/mm$^{3/2}$]
20	409	0.148	-
-120	583	0.134	1856
-150	681	0.128	1472

TABLE 4 - Material data used for the calculations in accordance with the theories of Chell, Curry.

DISCUSSION

It can be observed from table 3 that the present model gives reasonably accurate results. In Curry's article it is stated that Chell's and Curry's models are equivalent as these models yield almost the same results. This observation is not reflected in table 3. On the contrary, the results are quite different and no general conclusion can be drawn with respect to the accuracy of either of these models. The fact that Curry's model incorporates the strain hardening effects of the distinct loading steps obstructs a comparison of this model with Chell's model.
An important observation is the spread in the experimentally determined K_f-values as can be seen in table 2. This provides a strong reason to use a model for the prediction of the WPS-effect that has an accuracy which lies within the range of the spread of the measured K_f-values.
A final remark is made with respect to the fact that a WPS-effect ocurred in experiment E, in which the prestressing stress intensity factor K was lower then the low temperature toughness value K_{Ic} at -150°C. This was contrary to the expectation, according to Harrison and Fearnehough (2), who stated that the WPS-effect would occur when applying higher prestress levels than the low temperature fracture toughness level. This thesis is rejected by more quantitative WPS-models, such as the models of Chell and Curry and the present model.

CONCLUSIONS

1. The present model gives reliable results, especially at higher prestress loads.
2. Neglecting cumulative strain hardening effects as in Chell's and Curry's models, does not seriously

affect the results.

3. The present model involves much calculation effort and the determination of the required material parameters is quite time consuming. This makes the present model less suitable for a quick estimation of a WPS-effect. For this purpose Chell's model is excellent, as only the yield stresses at the temperatures of interest, as well as the low temperature K_{Ic}-value are needed.

ACKNOWLEDGEMENTS

Thanks are due to prof. ir. C. de Pater, ir. R.M.E.J. Spiering and ir. J. Maarse of Twente University of Technology for valuable discussions relating to the present model. Further I wish to acknowledge ir. C.E.P. van den Bergen from Koninklijke Shell Laboratorium Amsterdam for his help and advice regarding the experimental program, which was executed at that laboratory and ir. N.W.M. Verschuren who carried out the experiments.

REFERENCES

(1) Nichols R.W., British Welding Journal, Vol. 15, 1968, pp. 21-42, 75-84, 524-525.

(2) Harrison T.C. and Fearnehough. G.D., Trans. ASME, Jrnl. of Basic Engineering, 1972, pp. 373-376.

(3) Koshiga F., Practical Appl. of Fract. Mech. to Pressure Vessel Technology, 1971, paper C 50/71, pp. 168-174.

(4) Chell G.G. and Vitek V., Int. Jrnl. of Fracture, Vol. 13, 1977, RCR. 882-886

(5) Chell G.G., Haigh J.R. and Vitek V., Int. Jrnl. of Fracture, Vol. 17, 1981, pp. 61-81.

(6) Curry D.A., Int. Jrnl. of Fracture, Vol. 17, 1981, pp. 335-343.

(7) Ritchie R.O., Knott J.F. and Rice J.R., Jrnl. of the Mech. and Phys. of Solids, Vol 21, 1973, pp. 395-410.

(8) Curry D.A. and Knott J.F., Metal Science, Vol. 10,

1976, pp. 1-6.

(9) Besseling J.F., Jrnl. Appl. Mech., 1958, pp. 529-536.

(10) Nagtegaal J.C., Parks D.M. and Rice J.R., Comp. meth. in appl. mech. and. eng., Vol. 4, 1974, pp. 153-177.

(11) Bridgman P.W., Studies in large plastic flow and fracture, McGraw Hill, New York, 1952.

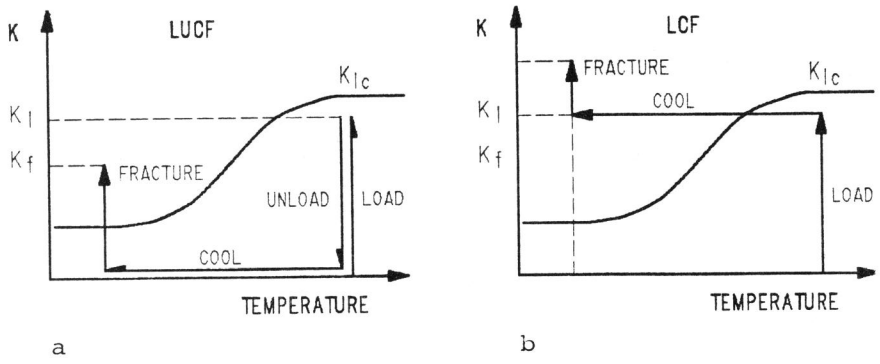

Figure 1 Warm prestressing terminology

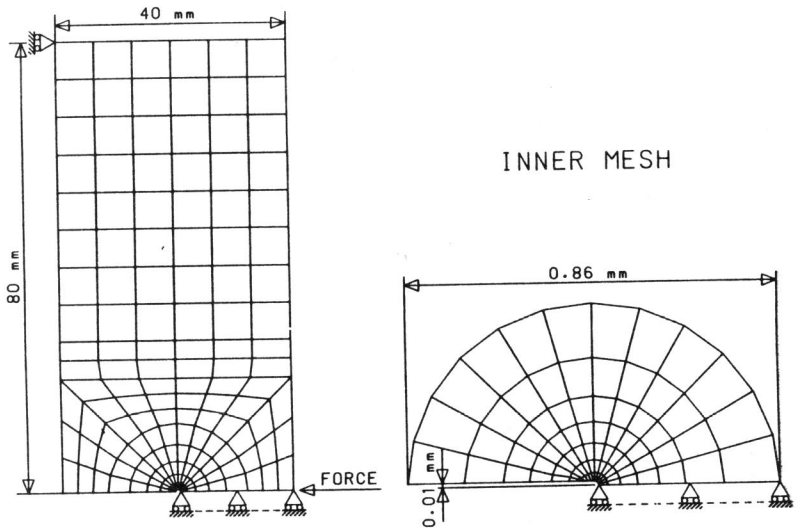

Figure 2 Finite element mesh for SENB

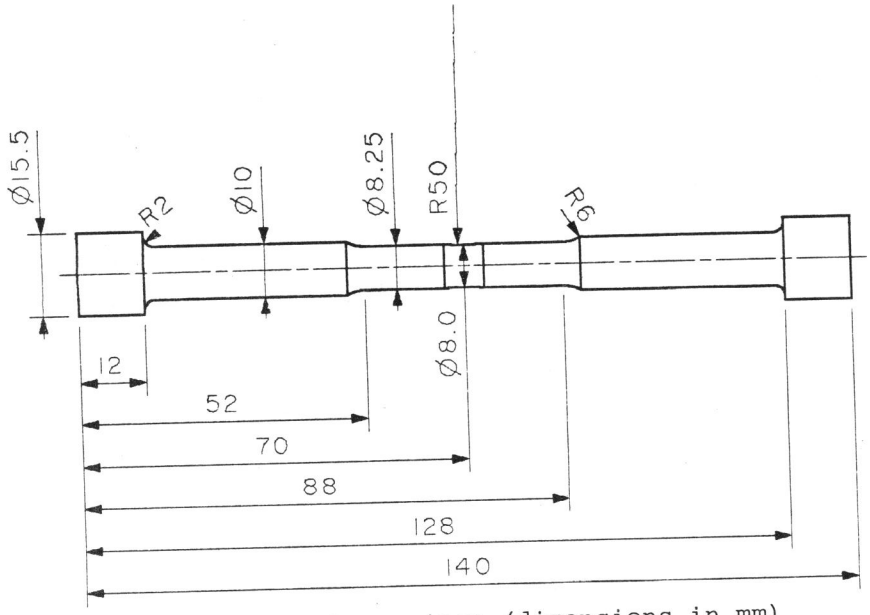

Figure 3 Tensile test specimen (dimensions in mm)

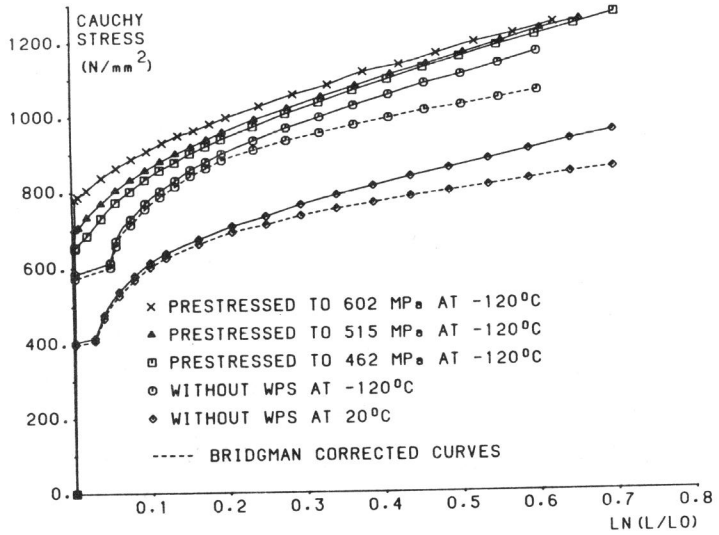

Figure 4 Experimental and Bridgman corrected strain hardening curves at 20°C and -120°C

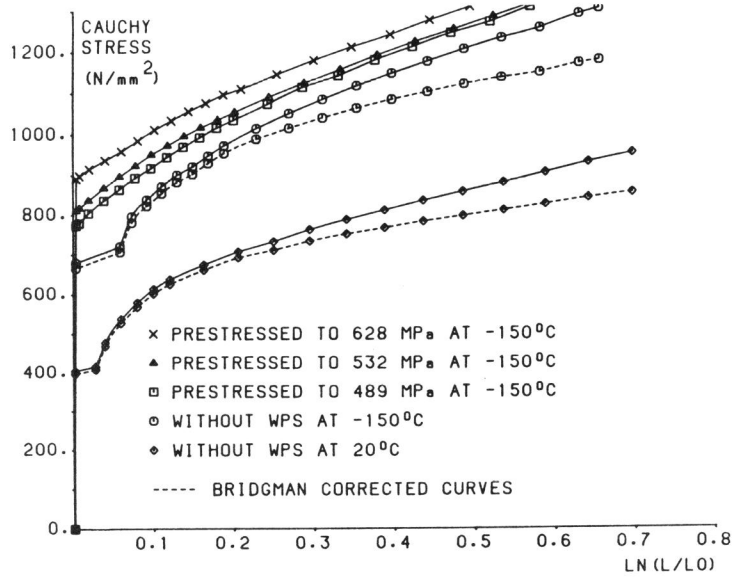

Figure 5 Experimental and Bridgman corrected strain hardening curves at 20°C and -150°C

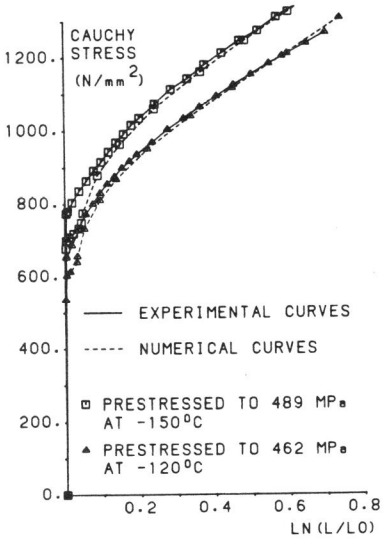

Figure 6 Experimental and numerical strain hardening curves

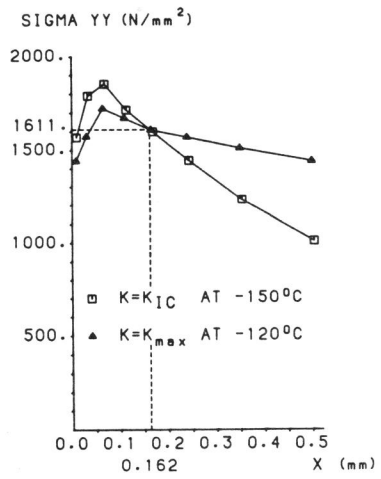

Figure 7 Maximum principal stress ahead of crack tip